Desalination and Water Treatment
www.deswater.com
doi: 10.1080/19443994.2016.1177733

57 (2016) 27419–27431
December

Taylor & Francis
Taylor & Francis Group

Modified adsorbent hydroxypropyl cellulose xanthate for removal of Cu^{2+} and Ni^{2+} from aqueous solution

Yongzhong Zhang[a], Chengcheng Luo[b], Hui Wang[b,*], Li Han[b], Chongqing Wang[b], Xuanmin Jie[b], Yong Chen[b]

[a]*School of Geosciences and Info-Physics, Central South University, Changsha 410083, Hunan, China, email: liuwuhui1968@163.com*
[b]*Key Laboratory of Resources Chemistry of Nonferrous Metals, School of Chemistry and Chemical Engineering, Ministry of Education, Central South University, Changsha 410083, Hunan, China, emails: ginoluo2011@163.com (C. Luo), huiwang1968@163.com (H. Wang), 179412502@qq.com (L. Han), 786252819@qq.com (C. Wang), jxmerish@gmail.com (X. Jie), 195073094@qq.com (Y. Chen)*

Received 24 June 2015; Accepted 7 March 2016

ABSTRACT

A modified adsorbent, namely hydroxypropyl cellulose xanthate (HCX), was synthesized for removal of heavy metal ions from aqueous solution. HCX was prepared by introducing xanthogenated groups, and the sulfur group in HCX was confirmed by scanning electron microscope, Fourier Transform Infrared, nuclear magnetic resonance, and ultraviolet-visible spectra. The sulfur group plays a significant role in chelating with heavy metal ions. Adsorption of copper and nickel ions by HCX was conducted, and the factors of adsorption time, temperature, adsorbent dose, and pH value were investigated. The removal rate of copper and nickel ions were up to 98 and 83% under the optimum condition, respectively. Adsorption isotherms indicated that Langmuir isotherm model had a better linearity and the maximum adsorption capacities of copper and nickel ions were 126.58 and 114.29 mg g^{-1} respectively, confirming that the affinity of metal ions onto sulfur-bearing groups was considerable.

Keywords: Hydroxypropyl cellulose xanthate; Xanthogenated groups; Adsorption; Heavy metal ions

1. Introduction

Heavy metals are widely used in various industries [1–3], and they have become a major threat to environment due to the undegradability and toxicity in living systems [4–8]. Numerous techniques have been developed for treating wastewater contaminated by heavy metal ions [9–12]. Conventional methods for removing heavy metal ions from aqueous solutions include chemical precipitation, oxidation, electrochemical treatment, solvent extraction, adsorption, ion exchange and membrane filtration technologies, etc. [13–19]. While these methods maybe cost-effective or ineffective and low removal rate when the concentration of metal ions in solution are in the range of 1–100 mg L^{-1} [20]. In recent years, adsorption technology is regarded as an attractive alternative for heavy metal ion removal from wastewater, and great efforts have been made to exploit new materials possessing properties such as low cost, high availability

*Corresponding author.

as well as efficient production process [1]. Agricultural wastes as adsorbents have manifested outstanding capabilities for removal of metal ions [21–24]. The hydroxyl groups in biomass chain bond with other groups and show a high affinity for heavy metal ions [25,26].

Hydroxypropyl cellulose (HPC) is a partially hydroxypropyl-substituted cellulose, in which some of the hydroxyl groups in the repeating glucose units have been hydroxypropylated with propylene oxide forming $–OCH_2CH(OH)CH_3$ groups. HPC often acts as an intermediate to synthesize other derivatives, and generally shows good reaction performance [27]. The introduction of hydroxypropyl groups into the cellulose backbone makes the macromolecules possess special properties, and this has found numerous applications in medicine, pharmacology, and membrane industry [28]. HPC, a rather heterogeneous polymer, is always used for emulsifying and thickening in non-dairy whipped topping [29], used as semipermeable membranes for drug delivery, and used in coating materials for reservoir or osmotic systems and excipients for matrix systems [30].

Most high molecular weight polysaccharides do not adsorb at the air/water interface [31]. However, HPC is a thick biopolymer having surface-active properties both at air/water and oil/water interfaces due to their mixed hydrophilic/hydrophobic structure [29,31]. G. Cavallaro and his coworkers studied the adsorption of thermosensitive polymer HPC onto the nanoclay surface in aqueous solution, and the adsorption equilibrium could explain the air/solution interface properties well [32]. Within this issue, HPC serving as a new synthetic material has a good solubility in water. It is easier to achieve a new environmental and high-efficiency adsorbent mainly for removal of heavy metal ions. The removal of Cu^{2+} and Ni^{2+} ions in aqueous solution was investigated, and the potential adsorption capacity of HCX in single system was determined.

2. Materials and methods

2.1. Materials

HPC powder used as raw material was purchased from Hebei Barilla biological Co., Ltd, China. All used chemicals in this work were of analytical reagent grade. The standard solution of Cu^{2+} and Ni^{2+} were prepared by dissolving $CuSO_4{\cdot}5H_2O$ and $Ni(NO_3)_2{\cdot}6H_2O$ in distilled water, respectively.

2.2. Methods

2.2.1. Characterization of adsorbent

Surface morphology analysis of the adsorbent was carried out using a scanning electronic microscope (SEM) (MIRA 3, TESCAN). Fourier Transform Infrared (FT-IR) spectra were recorded using KBr pellets with a NEXUS670 396 (Thermo Fisher Scientific) FT-IR spectrometer over the wavelength range 400−4,000 cm^{-1}. Ultraviolet spectra were recorded with an ultraviolet–visible (UV–vis) spectrophotometer. The ^1H nuclear magnetic resonance (NMR) spectra were recorded with 5-mm tubes in D_2O solution using AVANCE III HD 500 spectrometers. Sulfur content was measured by infrared carbon-sulfur analyzer (LECO, CS844).

2.2.2. Standard curve of copper ion and nickel ion

The concentration of heavy metal ions was measured by UV–vis spectra with UV-2450 spectrophotometer (Shimadzu Corporation, Japan) in pH 9–11 for Cu^{2+} and alkaline medium for Ni^{2+}. The content of Cu^{2+} was recorded in the range of 0.01–0.15 mg L^{-1} by UV spectrophotometric method at 440 nm, and Ni^{2+} was recorded in the range of 0.5–2 mg L^{-1} at 470 nm. The standard curves are exhibited below in Fig. 1. Linear correlation coefficient R^2 could be as high as 0.99988 and 0.99971 for Cu^{2+} and Ni^{2+}, respectively.

2.3. Synthesis of hydroxypropyl cellulose xanthate (HCX)

HPC (3 g) was alkalinized by 20 wt.% NaOH solution (60 mL) in a round-bottom flask under room temperature for 1 h. After this step, another 40 mL of NaOH solution was mixed into the slurry and then 3 mL of CS_2 was added dropwise at 30°C for 4 h, and stirring was needed for every stage. Afterward, 5 wt.% $MgSO_4$ solution (100 mL) was added into the flask for about 15 min to generate cellulose xanthate magnesium which is more stable than cellulose xanthate sodium [33]. After that, 300 mL of absolute ethyl alcohol was poured into the suspension, and the product was separated. After filtering the alcohol, the product was dissolved in about 10 mL of distilled water for dispersing agglomerate product. Purification of HCX by ethyl alcohol was repeated several times. Subsequently, the product was dried in vacuum oven at 40°C for 8 h. The mass obtained of HCX was 3.2 g and the sulfur content was recorded as 10.1%. The treatment procedure for preparation of HCX is illustrated in Fig. 2.

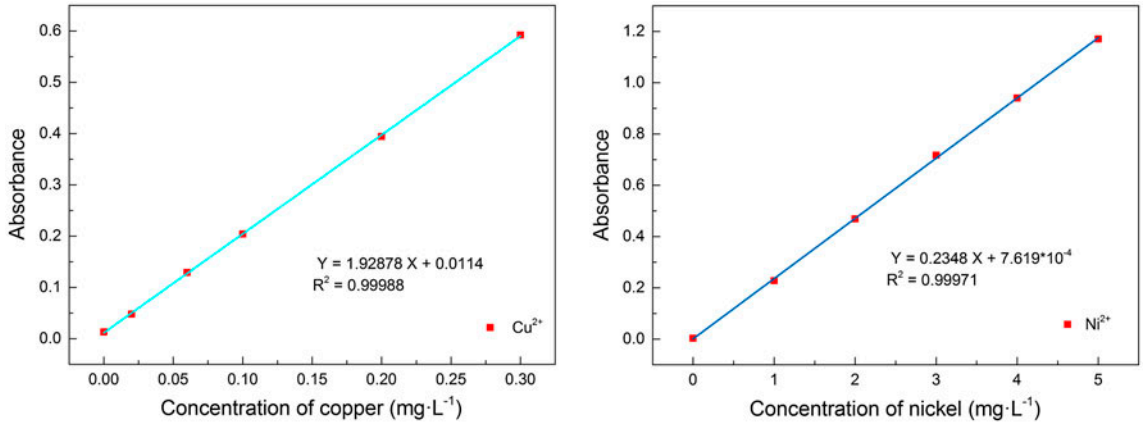

Fig. 1. Standard curves of Cu(II) and Ni(II).

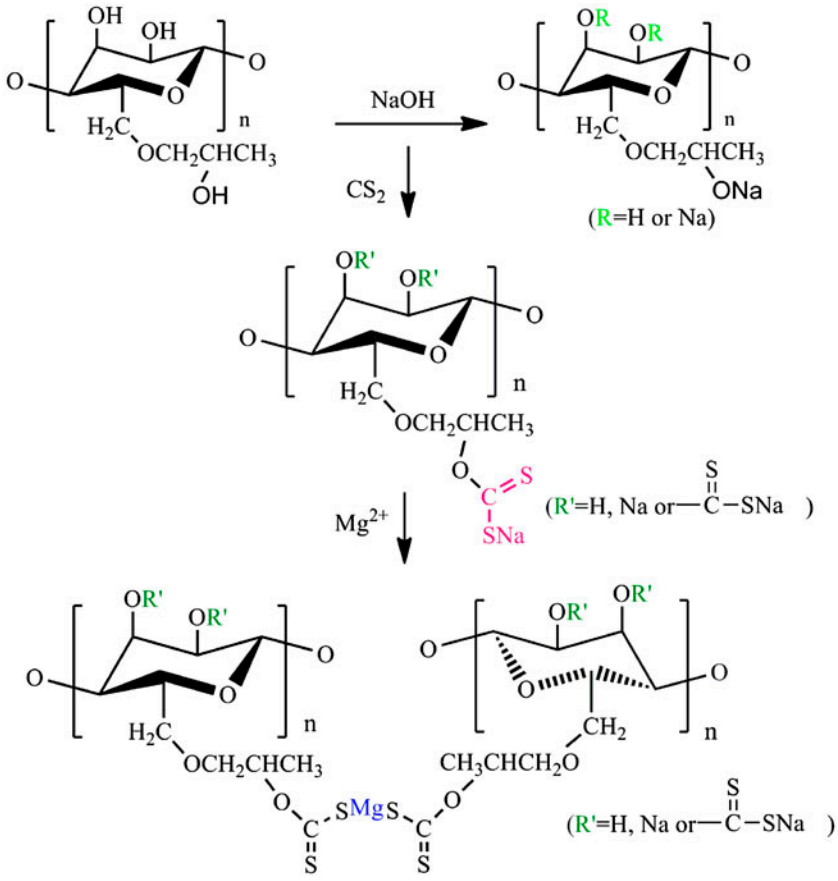

Fig. 2. Synthetic principles of Hydroxypropyl Cellulose Xanthate (HCX).

2.4. Heavy metal ions removal

The adsorption experiments were carried with aqueous solutions of Cu^{2+} and Ni^{2+} ions. The initial concentration of Cu^{2+} was 931.2 mg L^{-1} and Ni^{2+} was 954.1 mg L^{-1} before adsorption. The pH value of solution was adjusted with dilute H_2SO_4 and NaOH solution. The solution containing heavy metal ion was contacted with an accurately weighed amount of dried HCX in a conical flask with glass lid, and then kept under continuous oscillation in water-bathing thermostatic oscillator. After an appropriate time, the mixture

was centrifuged and the residual concentration of heavy metal ion in liquid phase was measured. Adsorption capacity and removal rate were evaluated by the following Eqs. (1) and (2):

$$q_e = \frac{(c_0 - c_1) \times V}{m} \quad (1)$$

$$R = \frac{(c_0 - c_1)}{c_0} \times 100\% \quad (2)$$

where q_e and R are the adsorption capacity and removal rate, respectively; c_0 and c_1 represent the initial and the residual heavy metal ion concentrations (mg L^{-1}), respectively. V is the volume of solution (mL), and m is the amount of HCX (g).

3. Results and discussion

3.1 Characterization

The SEM photographs of HPC and HCX are shown in Fig. 3. It is observed that the HPC consists of particles with diameter of 10−15 μm with a distinct smooth-faced surface due to the strong intra-molecular hydrogen bonds and the stereo-hindrance effect [34,35]. HCX possesses a porous structure on account of the corrosion by alkali solution and the xanthogenation by CS_2, which hamper the formation of inter- and intra-molecular hydrogen bonds. The porous structure would remarkably increase the available surface area of the adsorbent, giving rise to the enhancement of adsorption capacity.

The FT-IR spectra were recorded as a qualitative analysis to determine the main functional groups in the HPC and HCX. As presented in Fig. 4, the broad absorption band at 3,436 cm^{-1} corresponded to the characteristic stretching vibration of –OH, and the peak at 2,924 and 2,854 cm^{-1} corresponded to the C–H tensile vibration. The sharp band at 1,451 cm^{-1} corresponded to the deformation vibration of $–CH_2$ group [36], and the appearance of an absorption band located at 1,155 cm^{-1} was attributed to C–O–C stretching vibration of cellulose [37]. Some distinct changes were noted after xanthation of HPC. In addition, the adsorption peak at 1,646 cm^{-1} varied after the HPC treated by CS_2, and the presence of sulfur groups in the HCX had been identified by the appearance of new peaks at 1,104 cm^{-1} which corresponded to the vibration of C=S group [8].

Several reports pointed out that the cellulose xanthate was determined by measuring the ultraviolet absorbance at 303 nm [38–40]. Fig. 4 shows the absorption spectrum of cellulose xanthate in distilled water in the range 210–470 nm, where absorption maximum at 303 nm was observed. And it is obviously different from the spectrum of the HPC, for there was an intense peak at 223 nm. Aqueous solutions of HCX are unstable and easy to decompose. This instability is enhanced by decreasing hydroxide ion concentration and increasing temperature [38]. It is, therefore, advisable to keep the solution cold and read the absorbance of the solution as soon as possible after ion exchange.

The NMR spectra were seen by Fig. 5, and the proton chemical shifts of HCX were extremely different with HPC due to the treatment of CS_2. The reduplicative units in HPC were destroyed to be unordered, and thus the peaks in HCX were more tanglesome. The active hydrogen in hydroxyl will not be detected in D_2O, and only the signal peak of alkyl group and backbones in the spectra are observed.

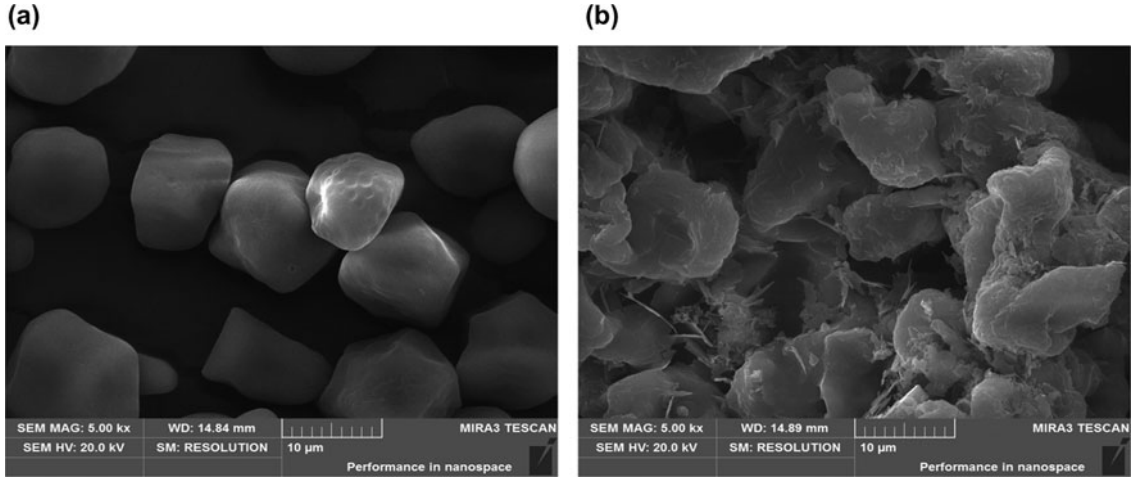

Fig. 3. SEM images of (a) HPC and (b) HCX.

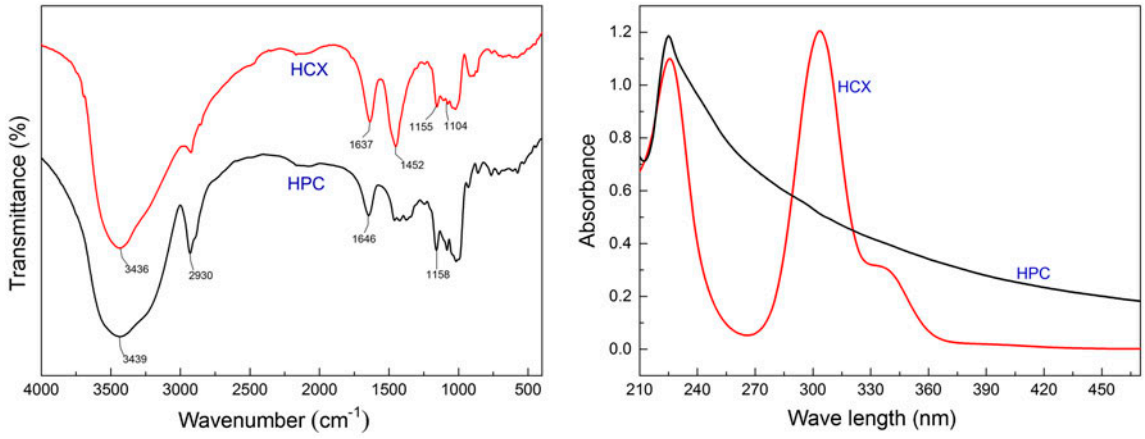

Fig. 4. FT-IR spectra and UV absorption spectra of HPC and HCX.

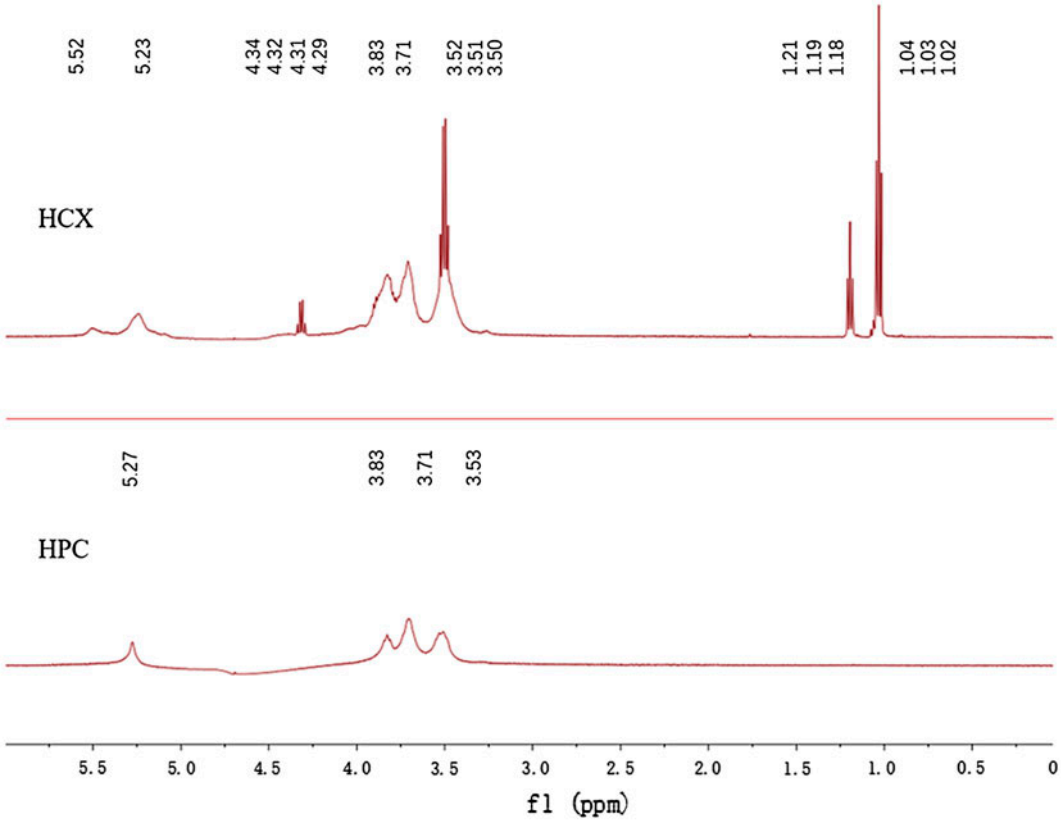

Fig. 5. The ^{1}H NMR spectra of HCX and HPC in D_2O solution. (The signal peak of D_2O was suppressed for featuring the peak of alkyl group and backbones).

3.2. Treatment of wastewater containing heavy metal ions

3.2.1. Effect of HCX consumption

The consumption of HCX for removal of Cu^{2+} and Ni^{2+} was investigated from 0.05 to 0.3 g 25 mL Cu^{2+} solution (931.2 mg L^{-1}) while Ni^{2+} solution (954.1 mg L^{-1}) was treated the same way. The pH value of Cu^{2+} solution was adjusted to about five while the pH value of Ni^{2+} solution was around six, oscillating under 30°C for 30 min. Then, centrifugation

was needed and metal ion concentration in the supernatant liquor was measured by UV–vis spectra. According to the principle of equivalent exchange ions, the theoretical amount of HCX is determined by the following Eq. (3) [41]:

$$M(\mathrm{HCX}) = 6.412 \times V \times \rho(\mathrm{Me}^{n+}) \times n/[M \times w(\mathrm{S})] \quad (3)$$

where V is the volume of heavy metal ion solution (L), $\rho(\mathrm{Me}^{n+})$ is the concentration of heavy metal ions (g L^{-1}), n is the metal ion valence, and M is the relative atomic mass, w(S) is sulfur content which was recorded as 10.1%. Theoretical amount gives a basis for the consumption of HCX.

The effect of HCX consumption on Cu^{2+} and Ni^{2+} removal was demonstrated in Fig. 6a. The concentration of heavy metal ions dropped obviously at first stage with the increment of HCX dose. This may be attributed to chemical modification which was expected to increase the binding sites in the surface area of the adsorbent and enhanced the adsorption capacity of HCX [28]. The residual heavy metal ions in aqueous solution no longer reduced until the adsorbent exceeded 0.2 g (about four times the theoretical amount), which indicated that adsorption had reached saturation point. At higher dosage, the adsorption capacity was low, and this may be due to overlapping of adsorption sites resulting in overcrowding of adsorbent particles. The residual concentration of Cu^{2+} and Ni^{2+} was 0.019–0.166 g L^{-1} in the end, and removal rate could reach 98 and 83%, respectively.

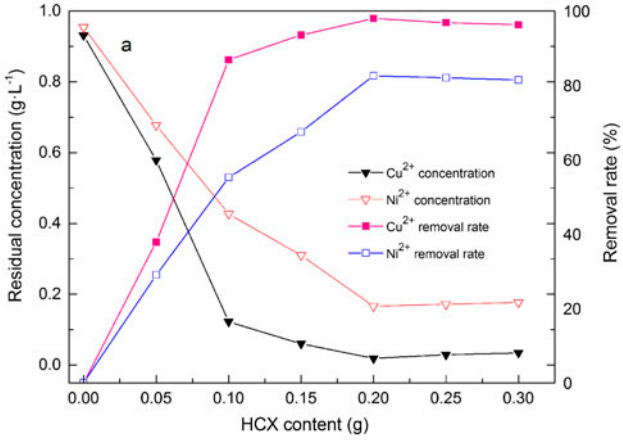

Fig. 6a. Effect of HCX content on the adsorption of Cu(II) and Ni(II). Conditions: contact time 30 min, solution pH 5.0 for Cu(II) and pH 6.0 for Ni(II).

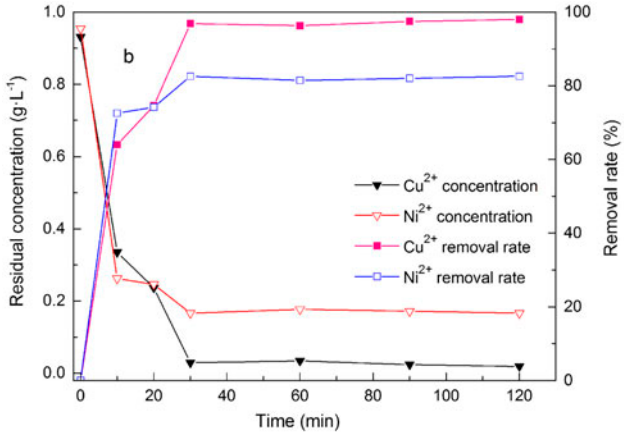

Fig. 6b. Effect of contact time on the adsorption of Cu(II) and Ni(II). Conditions: adsorbent dose 0.2 g, solution pH 5.0 for Cu(II) and pH 6.0 for Ni(II).

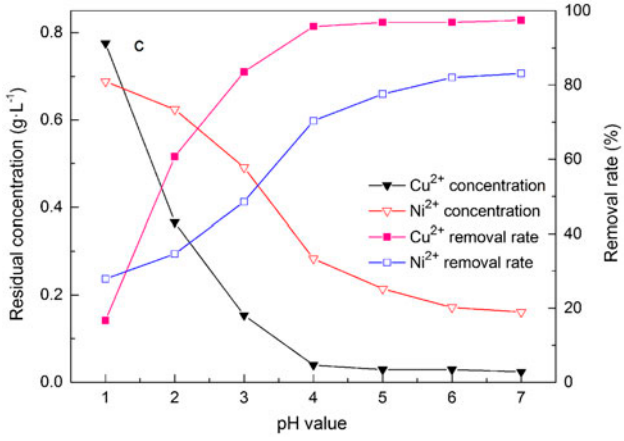

Fig. 6c. Effect of pH on adsorption of Cu(II) and Ni(II). Conditions: contact time 30 min, adsorbent dose 0.2 g.

3.2.2. Effect of time

To further assess the effect of time on the adsorption efficiency, general procedure was performed for 25 mL of solution (Cu^{2+} = 931.2 mg L^{-1}, Ni^{2+} = 954.1 mg L^{-1}) by varying the time from 10 to 120 min. The adsorption process was carried out at pH 5 for Cu^{2+} and 6 for Ni^{2+} with oscillating temperature 30˚C. It was found that HCX chelated with metal ions rapidly in the primary stage and 64% of Cu^{2+} and 72.5% of Ni^{2+} were removed within 10 min. According to Fig. 6b, the concentration of HCX slightly decreased with time, resulting in the decreased collision efficiency between molecules[42]. With time, a decrement of active sites was accompanied by a moderate decrease in metal ions, and the curve flattened out correspondingly.

3.2.3. Effect of pH

The metal speciation and ionization were affected by the pH value as well as the surface charge of the adsorbent. Thus, the metal ion adsorption was highly dependent on suitable pH value [43,44]. Fig. 6c manifested the result of heavy metal ion removal affected by the pH value of the solution. As it can be observed, the removal rate increased gradually until pH value rose to about 5, and then remained unchanged for both Cu^{2+} and Ni^{2+}. At low pH, the H^+ competition with heavy metal ions limits the uptake efficiency [45]. The higher pH value enhanced the removal rate of heavy metal ions, due to the ionization of xanthogenic acid groups [46]. As a result, the HPC xanthate (HCX) obtained the maximum adsorption capacity of $Cu^{2+}$and Ni^{2+} at pH near 5 and 6, respectively.

3.2.4. Effect of temperature

The effect of temperature on adsorption of Cu^{2+} and Ni^{2+} by HCX was studied using 1 g L^{-1} initial metal concentration at 30, 40, and 50℃. As presented in Fig. 7, it was found that the adsorption capacity decreased with increasing temperature. It indicated that the adsorption process was exothermic in nature. The thermodynamic parameters such as change in free energy (ΔG), enthalpy (ΔH), and entropy (ΔS) were calculated by the following equations [56,57]:

$$\Delta G = -RT \ln K_c \tag{4}$$

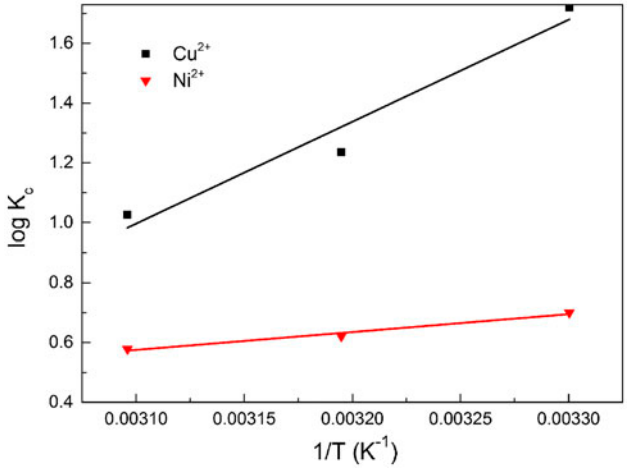

Fig. 7. Plot of log K_c vs. $1/T$ for estimation of thermodynamic parameter.

$$K_c = \frac{C_{Ae}}{C_e} \tag{5}$$

$$\log K_c = \frac{\Delta S}{2.30R} - \frac{\Delta H}{2.303RT} \tag{6}$$

where R is the gas constant, T is the temperature (ln K), K_c is the equilibrium constant, C_{Ae} is the equilibrium concentration of Cu^{2+} and Ni^{2+} on adsorbent (mg L^{-1}), and C_e is the equilibrium concentration of Cu^{2+} and Ni^{2+} in solution (mg L^{-1}).

The values of ΔH and ΔS were calculated from the slope and intercept of the linear plots of log K_c vs. $1/T$. The results are presented in Table 1. The negative values of ΔG indicated the spontaneous nature of adsorption. The ΔG values decreased with increase in temperature, indicating lesser adsorption capacity at higher temperatures [49]. The negative values of ΔH and ΔS confirmed the exothermic nature and the decreased randomness at the solid/solute interface during the adsorption of Cu^{2+} and Ni^{2+}, respectively.

3.3. Adsorption equilibrium

The Langmuir and the Freundlich adsorption models were calculated for better understanding the kinetics of adsorption of heavy metal ions [47].

3.3.1. Langmuir model

The main objective of Langmuir adsorption model was to estimate the capacity of uptaking metal ions. The linear form of the Langmuir isotherm is described by Eq. (7) [48]:

$$C_e/q_e = 1/k_L q_m + C_e/q_m \tag{7}$$

where C_e and q_e are the equilibrium metal ion concentration in the solution (mg L^{-1}) and the equilibrium metal ion concentration on the adsorbent (mg g^{-1}), k_L (L mg^{-1}) is the adsorption affinity constant which is connected to the energy of adsorption and q_m is the Langmuir saturated adsorption capacity of the adsorbent.

The enumerative Langmuir and affinity constants are shown in Table 1. A straight line between C_e and C_e/q_e was plotted with a slope of $1/q_m$ and an intercept of $1/k_L q_m$, which are shown in Figs. 8a and 8b. A further analysis of the Langmuir equation can be made on the basis of a dimensionless equilibrium parameter R_L. It is calculated by [35]:

Table 1
Thermodynamic parameters for the adsorption of Cu(II) and Ni(II) ions onto HCX

Metal	Temperature (°C)	Thermodynamics			
		ΔG (kJ mol^{-1})	ΔH (kJ mol^{-1})	ΔS (J mol^{-1} K^{-1})	R^2
Cu(II)	30	−9.98156	−65.344	−183.254	0.915
	40	−7.40266			
	50	−6.34475			
Ni(II)	30	−4.06142	−11.443	−24.424	0.957
	40	−3.72466			
	50	−3.5764			

$$R_L = \frac{1}{1 + k_L M c_0} \quad (8)$$

$$\ln q_e = \ln k_F + \frac{1}{n} \ln C_e \quad (9)$$

where c_0 (mmol L^{-1}) is the highest initial metal ion concentration, M is the molar mass of metal ions.

The values of R_L calculated are incorporated in Table 2. As the values of R_L are between 0 and 1, the adsorption system is favorable. And $R_L = 1$ represents linear adsorption, while the adsorption process is irreversible if $R_L = 0$ [50]. The dimensionless parameter R_L remained between 0.787 and 0.954 ($0 < R_L < 1$) consistent with the requirement for a favorable adsorption process.

3.3.2. Freundlich model

The Freundlich isotherm model is used to estimate the adsorption capacity (mg g^{-1}) and adsorption intensity. Its equation model can be expressed as Eq. (9). Fig. 9 showed the relationship between ln C_e and ln q_e which was linear with a slope of $1/n$ and an intercept of ln k_F.

where k_F is indicative of adsorption coefficient; n represents the adsorption intensity of Cu^{2+} and Ni^{2+} toward HCX.

The adsorption isotherm parameters evaluated for Cu^{2+} and Ni^{2+} are given in Table 2. The order for removal efficency in the case of aqueous solution is: $Cu^{2+} > Ni^{2+}$. The differences in removal efficency could be primarily due to their different affinity between various metal ions and cellulose xanthate salt, and the different mean adsorption energy that can influence the ionic states of the metal ions [51,52]. According to the results, it could be seen that the correlation coefficient (R^2) value of Langmuir model was closer to one compared with Freundlich model, revealing the linear Langmuir isotherm model had a better linearity. The applicability of the Langmuir isotherm suggested that the sorption was uniform and homogeneous as to the surface of the adsorbent as well as energy, resulting in the formation of a monolayer

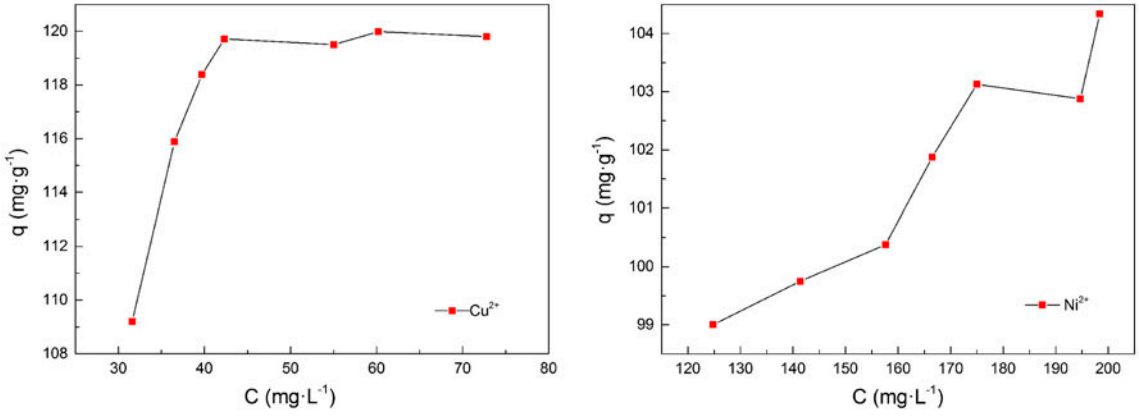

Fig. 8a. Adsorption isotherms of Cu(II) and Ni(II) for adsorption by HCX.

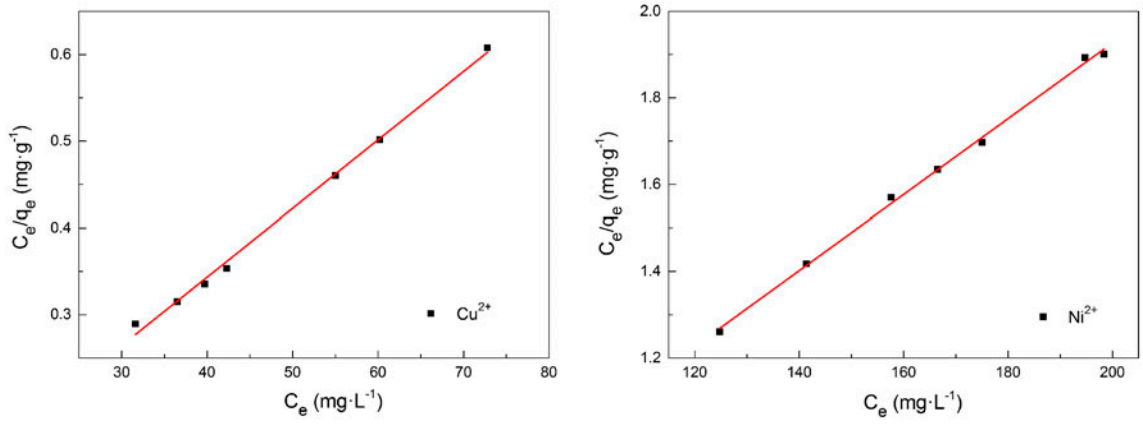

Fig. 8b. Linearized forms of Langmuir model for adsorption of Cu(II) and Ni(II) by HCX.

Table 2
Parameters of Langmuir and Freundlich isotherm constants for sorption of copper(II) and nickel(II) ions onto HCX at 30℃ for 30 min

	Langmuir adsorption isotherm				Freundlich adsorption isotherm		
	q_m (mg g^{-1})	k_L (L mg^{-1})	R^2	R_L	k_F	$1/n$	R^2
Cu^{2+}	126.58	0.29	0.996	0.787	99.11	0.045	0.90
Ni^{2+}	114.29	0.05	0.997	0.954	58.02	0.11	0.88

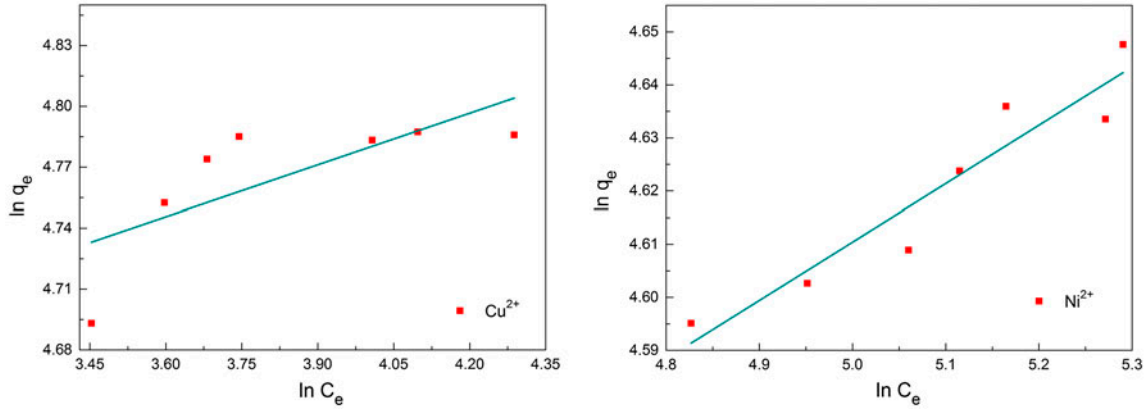

Fig. 9. Freundlich adsorption isotherms of Cu(II) and Ni(II) by HCX in single system.

coverage of Cu^{2+} and Ni^{2+}. Modified HCX possesses the characteristic of strong adsorption capacity. Comparison of HCX and modified HCX are showed in Table 3.

3.4. Adsorption kinetics

In order to better understand the kinetics of adsorption of heavy metal ions on HCX, it was studied for the efficiency of adsorption [45]. Kinetics data are modeled using pseudo-first-order model and pseudo-second-order model, the models were given by Eqs. (10) and (11). The pseudo-first-order equation was utilized to plot the data as $\ln(q_e - q_t)$ against t and pseudo-second-order equation was t/q_t against t. The sample plot for HCX at 30℃ for Cu(II) and Ni(II) ions is given in Fig. 10 and related parameters are shown in Table 4:

Table 3
Comparison of hydroxypropyl cellulose xanthate and modified hydroxypropyl cellulose xanthate on the study of metal ions adsorption

Cellulose xanthate	Metals	Adsorption capacities (mg g^{-1})	pH	Temperature (℃)
HCX	Cu(II), Ni(II)	126.58, 114.29	5.0–6.0	30
Insoluble bagasse xanthate [53]	Cu(II)	26.9	5.0 ± 0.1	18–21
Insoluble wood xanthate [53]	Cu(II)	27.8	5.0 ± 0.1	18–21
Orange peel xanthate [44]	Cu(II), Ni(II)	77.60, 15.45	5.0–5.5	25
Eichhornia crassipes root cellulose xanthate [54]	Cu(II)	98.37	4.5	25 ± 1
Modified sawdust xanthate [35]	Cu(II), Ni(II)	64.58, 40.86	6.0 ± 0.1	25
Xanthate-modified magnetic chitosan [8]	Cu(II)	34.5	6.0	30

$$\ln(q_e - q_t) = \ln q_e - k_1 t \quad (10)$$

$$t/q_t = 1/k_2 q_e^2 + t/q_e \quad (11)$$

where k_1, k_2, $q_{e,}$ and q_t are the pseudo-first-order adsorption rate constant (min^{-1}), the pseudo-second-order rate constant (g mg^{-1} min^{-1}), the adsorption amount by per unit adsorbent at equilibrium and at time t (mg g^{-1}), respectively.

From Fig. 10, it is obvious that the adsorption process could be well fitted by pseudo-second-order equation. This suggests the chemical adsorption is the rate limiting step. The mechanism involved in the adsorption of Cu^{2+} and Ni^{2+} onto HCX may be partly a result of the ion exchange followed by complexation. The HCX can bind transition metal ions by the formation of the coordination complex in which four sulfur atoms are associated with one divalent metal ion or two sulfur atoms associated with one divalent metal ion [2,42]. When cellulose xanthogenate dissolved in water, the active group could be hydrolyzed and ionized and was turned into xanthated ion in the end. The negative charge of *S* atom in —O—C(=S)—S⁻ disperses in a large space, thus displaying a negative electric field in a relative wide scope. So it could capture the cation, and tended to form the low solubility chelate [55].

Table 4
Pseudo-first-order and pseudo-second-order for the adsorption of metal ions on HCX at 30℃

Metal ions	Cu(II) ion	Ni(II) ion
First-order kinetics $\ln(q_e - q_t) = \ln q_e - k_1 t$		
k_1 ($\times 10^{-2}$ min^{-1})	5.38	3.86
R^2	0.979	0.965
Second-order kinetics $t/q_t = 1/k_2 q_e^2 + t/q_e$		
k_2 ($\times 10^{-3}$ g mg^{-1} min^{-1})	1.6	6.5
R^2	0.997	0.999

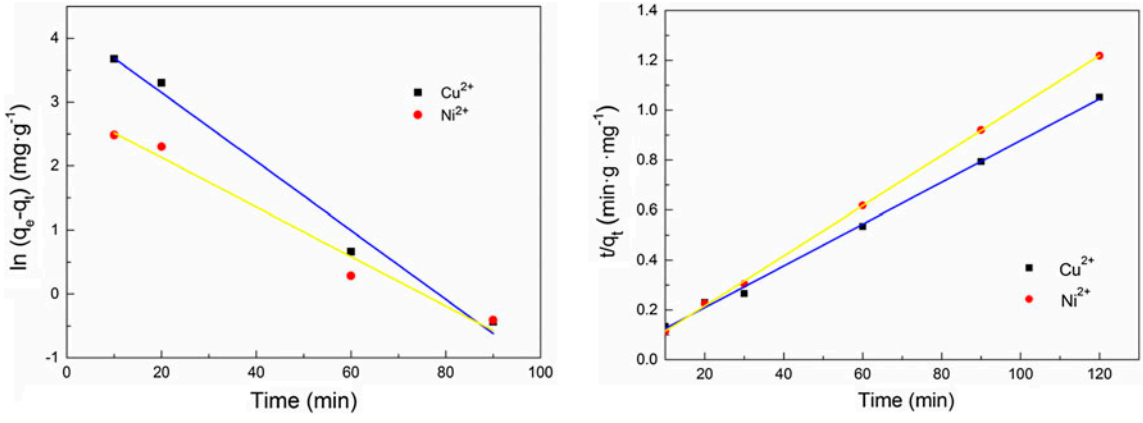

Fig. 10. Pseudo-first-order and pseudo-second-order kinetic model plots for adsorption of Cu(II) and Ni(II).

Because copper and nickel ions belong to transition metals, they have empty orbitals that can be occupied by extra electrons of *S* in HCX [42].

4. Conclusions

In this work, a new adsorbent HCX was synthesized and applied for adsorption of heavy metal ions. The modified cellulose demonstrated distinctive adsorption capability of copper and nickel ions. The optimum pH value in adsorption was about 5 and 6 for Cu^{2+} and Ni^{2+}. The adsorption equilibrium was achieved at 30 min and the adsorption saturation point was reached using 8 g HCX per liter heavy metal ion solution. The removal rate of copper and nickel ions were up to 98 and 83% under optimum conditions. Langmuir model correlated better with the adsorption mechanism. The maximum adsorption capacity of Cu^{2+} and Ni^{2+} were 126.58 and 114.29 mg g^{-1}, respectively. Kinetics studies indicated that the adsorption reaction followed pseudo-second-order model, and an ion exchange reaction followed by complexation mechanism might be involved in the adsorption. The results confirmed the potential of HCX as an effective adsorbent for the removal of heavy metal ions.

References

[1] F. Fu, Q. Wang, Removal of heavy metal ions from wastewaters: A review, J. Environ. Manage. 92 (2011) 407–418.

[2] S. Liang, X. Guo, N. Feng, Q. Tian, Isotherms, kinetics and thermodynamic studies of adsorption of Cu^{2+} from aqueous solutions by Mg^{2+}/K^{+} type orange peel adsorbents, J. Hazard. Mater. 174 (2010) 756–762.

[3] A. Mudhoo, V. Garg, S. Wang, Removal of heavy metals by biosorption, Environ. Chem. Lett. 10 (2012) 109–117.

[4] Z. Li, Z. Ma, T.J. van der Kuijp, Z. Yuan, L. Huang, A review of soil heavy metal pollution from mines in China: Pollution and health risk assessment, Sci. Total Environ. 468–469 (2014) 843–853.

[5] R. Bhat, in: S.A. Mansour (Ed.), Heavy metals of special concern to human health and environment, John Wiley & Sons, Inc., UK, 2014, pp. 213–233.

[6] K. Sharma, N. Basta, P. Grewal, Soil heavy metal contamination in residential neighborhoods in post-industrial cities and its potential human exposure risk, Urban Ecosyst. 18 (2015) 115–132.

[7] P. Wongsasuluk, S. Chotpantarat, W. Siriwong, M. Robson, Heavy metal contamination and human health risk assessment in drinking water from shallow groundwater wells in an agricultural area in Ubon Ratchathani province, Thailand, Environ. Geochem. Health 36 (2014) 169–182.

[8] Y. Zhu, J. Hu, J. Wang, Removal of Co^{2+} from radioactive wastewater by polyvinyl alcohol (PVA)/chitosan magnetic composite, Prog. Nucl. Energy 71 (2014) 172–178.

[9] G.O. Adams, P. Tawari-Fufeyin, E. Igelenyah, E. Odukoya, Assessment of heavy metals bioremediation potential of microbial consortia from poultry litter and spent oil contaminated site, Int. J. Environ. Biorem. Biodegrad. 2 (2014) 84–92.

[10] G.Z. Kyzas, E.A. Deliyanni, K.A. Matis, Graphene oxide and its application as an adsorbent for wastewater treatment, J. Chem. Technol. Biotechnol. 89 (2014) 196–205.

[11] S. Mahdavi, M. Jalali, A. Afkhami, Removal of heavy metals from aqueous solutions using Fe_3O_4, ZnO, and CuO nanoparticles, J. Nanopart. Res. 14(8) (2012) 1–18.

[12] K. Shakya, M.K. Chettri, T. Sawidis, Experimental investigations of five different mosses on accumulation capacities of Cu, Pb and Zn, Ecoprint: Int. J. Ecol. 90 (2008) 585–601.

[13] H.C. Chang, Y.H. Chen, A.T. Lo, S.S. Hung, S.L. Lin, I.N. Chang, J.C. Lin, Modified nanoporous membranes on centrifugal microfluidic platforms for detecting heavy metal ions, Mater. Res. Innovations 18 (2014) 685–690.

[14] L. Cui, J. Wu, H. Ju, Electrochemical sensing of heavy metal ions with inorganic, organic and bio-materials, Biosens. Bioelectron. 63 (2015) 276–286.

[15] F. Lin, D. Liu, S. Maiti Das, N. Prempeh, Y. Hua, J. Lu, Recent progress in heavy metal extraction by supercritical CO2 fluids, Ind. Eng. Chem. Res. 53 (2014) 1866–1877.

[16] C. Kazadi Mbamba, D.J. Batstone, X. Flores-Alsina, S. Tait, A generalised chemical precipitation modelling approach in wastewater treatment applied to calcite, Water Res. 68 (2015) 342–353.

[17] M. Naushad, A. Mittal, M. Rathore, V. Gupta, Ion-exchange kinetic studies for Cd(II), Co(II), Cu(II), and Pb (II) metal ions over a composite cation exchanger, Desalin. Water Treat. 54 (2014) 2883–2890.

[18] S. Sohi, R. Cleat, M. Graham, A. Cross, Long-term balance in heavy metal adsorption and release in biochar derived from sewage sludge, in: EGU General Assembly Conference Abstracts, 2014, pp. 15624.

[19] W.S. Wan Ngah, L.C. Teong, M.A.K.M. Hanafiah, Adsorption of dyes and heavy metal ions by chitosan composites: A review, Carbohydr. Polym. 83 (2011) 1446–1456.

[20] S.S. Ahluwalia, D. Goyal, Microbial and plant derived biomass for removal of heavy metals from wastewater, Bioresour. Technol. 98 (2007) 2243–2257.

[21] C.S. Gray, S.E. Burns, J.D. Griffith, The use of natural zeolites as a sorbent for treatment of dissolved heavy metals in stormwater runoff, Bridges 10 (2014) 3978–3987.

[22] D. Mani, C. Kumar, Biotechnological advances in bioremediation of heavy metals contaminated ecosystems: An overview with special reference to phytoremediation, Int. J. Environ. Sci. Technol. 11 (2014) 843–872.

[23] M.A. Martín-Lara, G. Blázquez, M.C. Trujillo, A. Pérez, M. Calero, New treatment of real electroplating wastewater containing heavy metal ions by adsorption onto olive stone, J. Cleaner Prod. 81 (2014) 120–129.

[24] S.M.A.E.H. Mosa, Adsorption of some heavy metals and (Mg, Ca) ions from aqueous solutions by using

different environmental residuals as a cheap adsorbents at optimum conditions, Science 2 (2014) 1–5.
[25] D. Roy, M. Semsarilar, J.T. Guthrie, S. Perrier, Cellulose modification by polymer grafting: A review, Chem. Soc. Rev. 38 (2009) 2046–2064.
[26] W. Zhou, X. Ge, D. Zhu, A. Langdon, L. Deng, Y. Hua, J. Zhao, Metal adsorption by quasi cellulose xanthogenates derived from aquatic and terrestrial plant materials, Bioresour. Technol. 102 (2011) 3629–3631.
[27] X. Xu, X. Zhuang, B. Cheng, J. Xu, G. Long, H. Zhang, Manufacture and properties of cellulose/O-hydroxyethyl chitosan blend fibers, Carbohydr. Polym. 81 (2010) 541–544.
[28] C.D. Nechifor, A. Barzic, I. Stoica, V. Cloşca, D.O. Dorohoi, Study on glucose release ability from hydroxypropyl cellulose films, Polym. Bull. 72 (2015) 549–563.
[29] S. Mezdour, G. Cuvelier, M.J. Cash, C. Michon, Surface rheological properties of hydroxypropyl cellulose at air–water interface, Food Hydrocolloids 21 (2007) 776–781.
[30] P. Ledwon, J.R. Andrade, M. Lapkowski, A. Pawlicka, Hydroxypropyl cellulose-based gel electrolyte for electrochromic devices, Electrochim. Acta 159 (2015) 227–233.
[31] S. Mezdour, A. Lepine, P. Erazo-Majewicz, F. Ducept, C. Michon, Oil/water surface rheological properties of hydroxypropyl cellulose (HPC) alone and mixed with lecithin: Contribution to emulsion stability, Colloids Surf. A 331 (2008) 76–83.
[32] G. Cavallaro, G. Lazzara, S. Milioto, Aqueous phase/nanoparticles interface: Hydroxypropyl cellulose adsorption and desorption triggered by temperature and inorganic salts, Soft Matter 8 (2012) 3627–3633.
[33] F.J. Wang, H.Y. Hao, Z.Q. Shao, H.M. Tan, W.Z. Tian, Preparation and application of bagasse explosion treatment and xanthating, J. Cellul. Sci. Technol. 11 (2003) 29–34.
[34] M.H. Beyki, M. Bayat, S. Miri, F. Shemirani, H. Alijani, Synthesis, characterization, and silver adsorption property of magnetic cellulose xanthate from acidic solution: Prepared by one step and biogenic approach, Ind. Eng. Chem. Res. 53 (2014) 14904–14912.
[35] L. Xia, Y.X. Hu, B.H. Zhang, Kinetics and equilibrium adsorption of copper(II) and nickel(II) ions from aqueous solution using sawdust xanthate modified with ethanediamine, Trans. Nonferrous Met. Soc. China 24 (2014) 868–875.
[36] G. Guibaud, N. Tixier, A. Bouju, M. Baudu, Relation between extracellular polymers' composition and its ability to complex Cd, Cu and Pb, Chemosphere 52 (2003) 1701–1710.
[37] J. Shi, H. Luo, J. Hu, D. Xiao, Y. Tu, B. Lin, X. Liang, Removal of Cr^{6+} ions by cross-linked cassava xanthate from aqueous solution, Adv. Polym. Tech. 33 (2014) 21424–21429.
[38] J.P. Dux, L.H. Phifer, Determination of xanthate sulfur in viscose, Anal. Chem. 29 (1957) 1842–1845.
[39] L.H. Phifer, L.B. Ticknor, Reaction of formaldehyde with cellulose xanthate, J. Appl. Polym. Sci. 9 (1965) 1055–1065.
[40] H.Y. Zeng, W. Li, Z.M. Li, Studise on the preparation and characterization of water soluble cellulose xanthate and its application in the recovery of gold, J. Cellul. Sci. Technol. 2 (1993) 53–59.
[41] J.H. Shi, B.F. Lin, D.S. Xiao, J.W. Hu, study of adsorption of chromium (VI) from aqueous solution by crosslinked cassava residue xanthate, Appl. Chem. Ind. 41 (2012) 609–612.
[42] Q.H. Li, C.B. Sun, synthesis and application of sawdust cellulose xanthate in treatment of nickle metal wastewater, Jiangsu Environ. Sci. Technol. 17 (2005) 11–13.
[43] H.T. Kim, K. Lee, Application of insoluble cellulose xanthate for the removal of heavy metals from aqueous solution, Korean J. Chem. Eng. 16 (1999) 298–302.
[44] S. Liang, X.Y. Guo, N.C. Feng, Q.H. Tian, Effective removal of heavy metals from aqueous solutions by orange peel xanthate, Trans. Nonferrous Met. Soc. China 20 (2010) s187–s191.
[45] T.S. Anirudhan, S.S. Sreekumari, Synthesis and characterization of a functionalized graft copolymer of densified cellulose for the extraction of uranium(VI) from aqueous solutions, Colloids Surf. A 361 (2010) 180–186.
[46] J. Duan, Q. Lu, R. Chen, Y. Duan, L. Wang, L. Gao, S. Pan, Synthesis of a novel flocculant on the basis of crosslinked Konjac glucomannan-graft-polyacrylamide-co-sodium xanthate and its application in removal of Cu^{2+} ion, Carbohydr. Polym. 80 (2010) 436–441.
[47] G.P. Jeppu, T.P. Clement, A modified Langmuir-Freundlich isotherm model for simulating pH-dependent adsorption effects, J. Contam. Hydrol. 129–130 (2012) 46–53.
[48] G.Z. Kyzas, P.I. Siafaka, E.G. Pavlidou, K.J. Chrissafis, D.N. Bikiaris, Synthesis and adsorption application of succinyl-grafted chitosan for the simultaneous removal of zinc and cationic dye from binary hazardous mixtures, Chem. Eng. J. 259 (2015) 438–448.
[49] V.N. Tirtom, A. Dinçer, S. Becerik, T. Aydemir, A. Çelik, Comparative adsorption of Ni(II) and Cd(II) ions on epichlorohydrin crosslinked chitosan–clay composite beads in aqueous solution, Chem. Eng. J. 197 (2012) 379–386.
[50] R. Bazargan-Lari, M. Bahrololoom, A. Nemati, Sorption behavior of Zn (II) ions by low cost and biological natural hydroxyapatite/chitosan composite from industrial waste water, J. Food Agric. Environ. 9 (2011) 892–897.
[51] A. Kumar, N.N. Rao, S.N. Kaul, Alkali-treated straw and insoluble straw xanthate as low cost adsorbents for heavy metal removal–preparation, characterization and application, Bioresour. Technol. 71 (2000) 133–142.
[52] A.H. Chen, S.C. Liu, C.Y. Chen, C.Y. Chen, Comparative adsorption of Cu(II), Zn(II), and Pb(II) ions in aqueous solution on the crosslinked chitosan with epichlorohydrin, J. Hazard. Mater. 154 (2008) 184–191.
[53] S. Chakraborty, V. Tare, Role of various parameters in synthesis of insoluble agrobased xanthates for removal of copper from wastewater, Bioresour. Technol. 97 (2006) 2407–2413.
[54] L. Tan, D. Zhu, W. Zhou, W. Mi, L. Ma, W. He, Preferring cellulose of eichhornia crassipes to prepare xanthogenate to other plant materials and its adsorption properties on copper, Bioresour. Technol. 99 (2008) 4460–4466.

[55] H.S. Hou, Removal of heavy metal ions by sawdust yellow chlorogenic acid salt, Electroplat, Pollut. Control 5 (1988) 11–15.
[56] K. Fujiwara, A. Ramesh, T. Maki, H. Hasegawa, K. Ueda, Adsorption of platinum (IV), palladium (II) and gold (III) from aqueous solutions onto l-lysine modified crosslinked chitosan resin, J. Hazard. Mater. 146 (2007) 39–50.
[57] M. Rafatullah, O. Sulaiman, R. Hashim, A. Ahmad, Adsorption of copper (II), chromium (III), nickel (II) and lead (II) ions from aqueous solutions by meranti sawdust, J. Hazard. Mater. 170 (2009) 969–977.